IEEE Access
Multidisciplinary | Rapid Review | Open Access Journal

Received February 8, 2020, accepted February 22, 2020, date of publication February 27, 2020, date of current version March 11, 2020.

Digital Object Identifier 10.1109/ACCESS.2020.2976823

Angularly Stable Bandpass Frequency Selective Surface Based on Metasurface

MEIJUN QU[1], BIN LI[2], SIYANG SUN[3], AND SHUFANG LI[1], (Senior Member, IEEE)

[1]School of Information and Communication Engineering, Beijing University of Posts and Telecommunications, Beijing 100876, China
[2]International Department, The State Radio Monitoring Center Testing Center, Beijing 100041, China
[3]China Telecommunication Technology Labs, China Academy of Information and Communications Technology, Beijing 100191, China

Corresponding author: Siyang Sun (sunsiyang@caict.ac.cn)

This work was supported by the National Natural Science Foundation of China under Grant 61427801 and Grant 61601040.

ABSTRACT A novel bandpass frequency selective surface (FSS) working at 2.4 GHz is proposed in this paper based on metasurface with independent-polarization, wide rejection band and good angular stability. The 10-dB upper stopband could cover 3.35-9.4 GHz with a fractional bandwidth of 94.9%. In addition, the filtering response could remain stable under different polarizations and incidence angles. Parameter analysis and equivalent circuit model are illustrated to explain the resonance behavior of the proposed FSS. It is demonstrated that the lower resonant point in the stopband could be tuned independently by changing the length of small rectangular patches in the top layer. While the higher resonant point could be changeable independently by adjusting the diameter of circular gap in the bottom layer. A prototype of the proposed FSS is fabricated and its simulated results are coincided with measurements.

INDEX TERMS Angular stability, FSS, metasurface, polarization-independent, wide stopband.

I. INTRODUCTION

FSS is a kind of periodic artificial electromagnetic surface. Due to its low loss, low cost, low profile and easy conformal, FSS has been widely used in numerous areas such as radomes [1]–[4] rasorbers [5]–[8], antenna reflectors [9]–[12], spatial filters [13]–[16], as well as electromagnetic band gap materials [17]–[19].

The operating principle of the traditional FSS is based on resonance. Thus, the size of the FSS element is quite large, about half wavelength. Over the past several years, FSS with miniaturized unit-cell size has been investigated intensively. On the one hand, in practice application, especially in low-frequency communication system, there are space constraints. By using miniaturized FSS unit, more units can be laid out in limited space, which could improve the performance of FSS. On the other hand, miniaturized FSS could improve its angular stability under oblique incidence because the grating lobe phenomenon can be reduced. In [20], a single-polarized miniaturized 3-D bandpass FSS using stepped impedance resonators is proposed. It exhibits stable frequency response under oblique incidence of angles up to 60°. Another miniaturized-element bandpass FSS is reported in [21]. This design using 3-D printing technology to selectively regulate the dielectric thickness that results in a reduced resonance frequency. The angular stability under oblique incidence can reach 75°. Nevertheless, compared with the conventional 2-D FSS, in addition to the higher cost, there are more difficulties in fabrication and implementation. Loading lumped components is an efficient method to achieve ultraminiaturized unit-cell. A miniaturized FSS using lumped inductors and capacitors has been proposed in [22]. The measured insertion loss of passband is 1 dB. The loss is mainly caused by the effect of the welding point in the FSS prototype. Moreover, the values of lumped components are always fixed and discontinuous. In [23], loading with capacitive structures rather than welding capacitance components directly, it could miniaturize FSS unit-cell size successfully. The angular stability under oblique incidence can be up to 60°. Nowadays, metasurface has attracted much attention due to its flexible regulation of electromagnetic waves. The metasurface element is less than one tenth of a wavelength. Therefore, it can be suitable for miniaturization of FSS.

In addition to miniaturization, due to the increasing complexity of electromagnetic in the environment, bandpass FSS with wide out-of-band rejection gains more and more attention. However, most aforementioned designs cannot achieve miniaturization and wide stopband simultaneously. A class

The associate editor coordinating the review of this manuscript and approving it for publication was Chan Hwang See.

of bandpass FSS with improved out-of-band rejection is presented in [24] by using stacked slotlines. Incident EM waves can propagate along the special slotlines, thus leading to the desired bandpass filtering response. Yet multilayer structure will increase the profile height of FSS. In [25], By cascading 2-D loop arrays, a quasi-elliptic bandpass FSS is presented. In the upper stopband, two transmission zeros are produced. Nevertheless, the two transmission zeros cannot be adjusted independently. In [26], one FSS with zeros adjustable quasi-elliptic response is designed. There are two transmission zeros in the upper stopband which could be tuned independently by changing the size of the hollow metal pipe array and metal disk array. It should be mentioned that the author in [26] indicates that the FSS is not suitable for radome exposed to oblique incident waves. Though the above analysis, our purpose is to design a low profile miniaturized FSS based on metasurface with high angular stability to against the generation of grating lobe. At the same time, the proposed FSS should have wide stopband while the transmission zeros can be adjusted independently.

II. FSS BASED ON METASURFACE AND ITS PRINCIPLE

Fig. 1 shows the configuration of the proposed FSS unit which is constructed on Rogers 4350 substrate with relative permittivity constant of 3.66, thickness of 30 mil and dielectric loss of 0.004. The top layer of the proposed FSS consists of a rectangular ring and four rectangular patches connected by eight metallic strips. While the bottom layer is a square embedded a circular gap in the center. The proposed FSS is polarization independent due to its symmetrical structure.

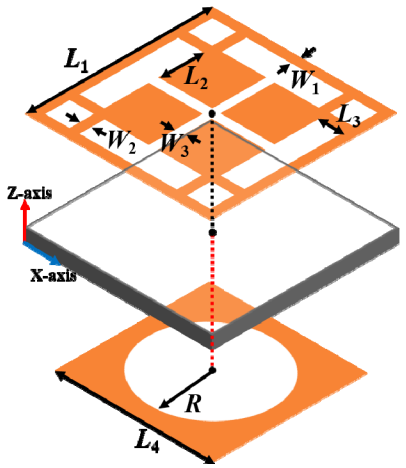

FIGURE 1. Configuration of the proposed FSS unit (Geometrical parameters: $L_1 = 9.45$ mm, $L_2 = 3.62$ mm, $L_3 = 0.63$ mm, $L_4 = 7.6$ mm, $W_1 = 0.1$ mm, $W_2 = 0.3$ mm, $W_3 = 0.15$ mm, $R = 2.9$ mm).

The design of FSS unit-cell must be appropriate to prevent the appearance of grate lobes. Grate lobe is the transmission or scattering of electromagnetic energy in an undesirable direction when the unit cycle is relatively large. The general criterion for suppressing grating lobes is: for vertical incidence, the unit-cell size should be less than one wavelength; for oblique incidence, the unit-cell size should be less than half wavelength. In other words: the smaller the unit-cell size, the more conducive it is to inhibit the generation of the grate lobes. It is also conducive to miniaturization as well. The proposed FSS unit-cell is 0.0756 $\lambda_0 \times 0.0756$ λ_0 (λ_0 is the free-space wavelength corresponding the resonance frequency − 2.4 GHz). The key to achieving wide angular bandwidth is to design a FSS unit with a small size. By introducing small patches and slots, inductance and capacitance are actually introduced. The larger the inductance and capacitance, the resonance frequency will shift to a lower frequency range, thus resulting in miniaturization.

Figs. 2(a-b) illustrate the transmission coefficients of the proposed FSS with different values of R and L_2 under normal incidence. It is clear that there are two transmission zeros. Though parameter analysis, it is found that the higher resonance frequency of transmission coefficients can be shifted to lower frequency as the value of R increases. While the lower resonance frequency almost remains unchanged. The lower resonance frequency can move towards the higher frequency when the value of L_2 is increased. The higher resonance frequency is stable at this time. Therefore, the

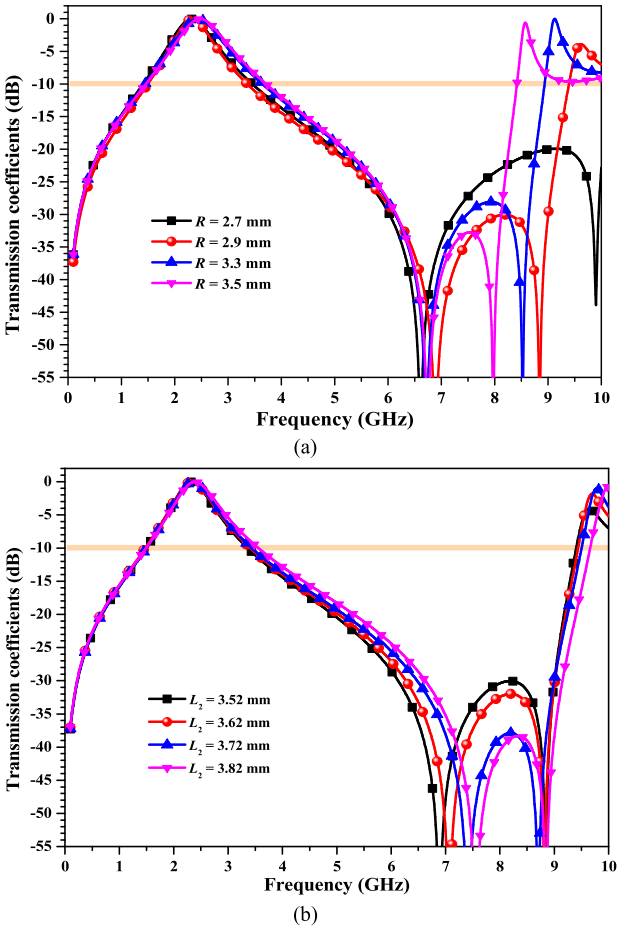

FIGURE 2. Transmission coefficients of the proposed FSS with different values of (a) R and (b) L_2 under normal incidence.

two transmission zeros can be adjusted independently in a certain frequency range by changing the value of only one parameter. This advantage is very helpful for debugging in actual measurement. The existence of two transmission zeros widens the upper stopband and improves the selectivity of the proposed FSS. The operating frequency in the passband remains unchanged when the values of R and L_2 are various.

To further explain the operating mechanism of the proposed FSS, equivalent circuit is studied and plotted in Fig. 3(a). Z_0 is the characteristic impedance (377 ohm) of the free space. The rectangular ring in the upper layer could be modeled as an inductance L_0. While four rectangular patches and eight metallic strips can be equivalent to series capacitance C_1 and inductance L_1 due to the existence of gaps. The bottom layer is a square embedded a circular gap in the center. Therefore, it can be seen as the series capacitance C_2 and inductance L_2. Since the substrate adopted in the proposed design is very thin, only 30 mil, there is a capacitor C_0 between the metal structures of the upper and lower surfaces. The equivalent circuit parameters of the proposed FSS: $L_0 = 6.7$ nH, $C_0 = 0.35$ pF, $C_1 = 0.42$ pF, $L_1 = 1.29$ nH, $C_2 = 0.3$ pF, $L_2 = 1.1$ nH.

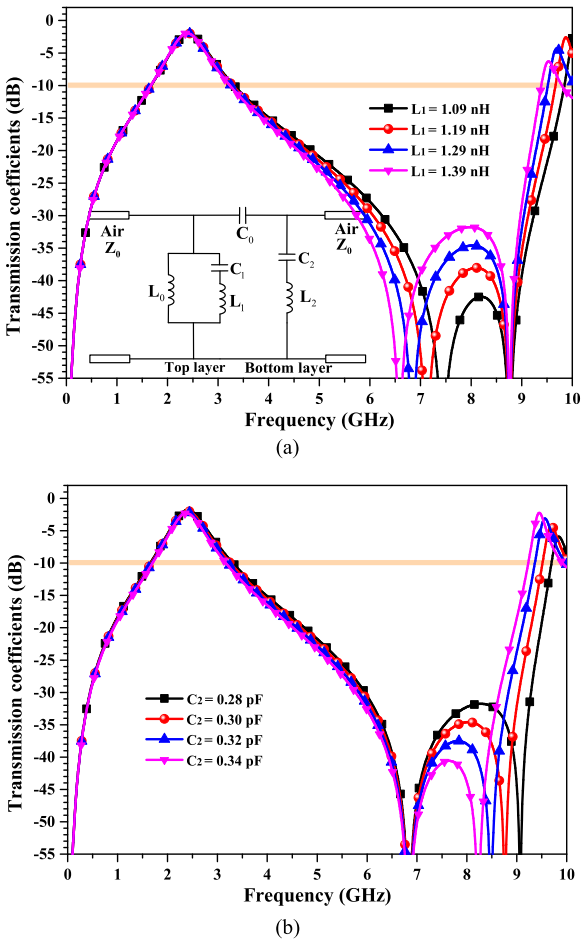

FIGURE 3. Transmission coefficients of the proposed FSS with different values of (a) inductance L_1 and (b) capacitance C_2.

From the aforementioned parameter analysis, it is known that the two resonance frequencies in the stopband can be adjusted independently while the passband remains unchanged. We simulate the equivalent circuit of the proposed FSS in ADS (Advanced design system). The corresponding simulated results are illustrated in Figs. 3(a-b). When the value of inductance L_1 (a parameter in the top layer) is changed from 1.09 to 1.39 nH, it is observed that the lower resonant point moves towards lower frequency band. And the upper resonant point has hardly changed. When the value of capacitance C_2 (a parameter in the bottom layer) is increased from 0.28 to 0.34 pF, it is found that the higher resonant point moves towards lower frequency band. While the change in the value of C_2 has no effect on the lower resonant point. These two resonant points could also be tuned independently from the simulated results in ADS. It further proves the feasibility of the proposed design.

It should be mentioned that this equivalent circuit in this paper is extracted under the normal incidence. At this point, the input impedance of this equivalent circuit should be matched to 377 ohm in free space. When the incident wave is inclined, the wave impedances of TE and TM modes would change with different angles of incidence. If the wave impedance corresponding to the TE mode or TM mode deviates too much from 377 ohms, the equivalent circuit at this time is invalid, and the proposed FSS cannot work normally.

III. SIMULATED AND EXPERIMENTAL RESULTS

To describe the resonant mechanism, induced current disribution at transmission pole and transmission zeros of the proposed FSS for transverse electric (TE) polarization are shown in Fig. 4. The color of the arrow represents the intensity and direction of arrow indicates the current flow. The currents are mainly distributed on the rectagular loops (black box) at 2.4 GHz in the top layer. While the currents cancel out at the bottom layer. Therefore, the period of the unit-cell controls the position of the transmission pole. At 6.84 GHz, the currents are mainly concentrated in the corners (blue box) of the unit-cell at the top layer. Thus, the first transmission zero is determined by the parameter L_2. The currents at 8.76 GHz are focused on the circular slot (black circular) at the second layer. Namely, parameter R_2 is the key factor which could affect the location of the second transmission zero.

The oblique property for TE and TM polarizations is investigated in Figs. 5(a-b). It is observed that the passband and stopband of the proposed FSS are quite stable with 60° oblique incidence both in the case of TE and TM polarizations. Nevertheless, even with a narrow bandwidth under TE polarization, the designed FSS can still work at 80°. The -3 dB bandwidth is decreased for the TE polarization and increased for the TM polarization when the incident angle is increased. This is due to that the increased incidence angle θ leads to a greater wave impedance $Z_{TE} = Z_0/\cos\theta$ for the TE polarization, and a smaller wave impedance $Z_{TM} = Z_0 \times \cos\theta$ for the TM polarization [27]. The simulated results demonstrate that the proposed FSS has merits of

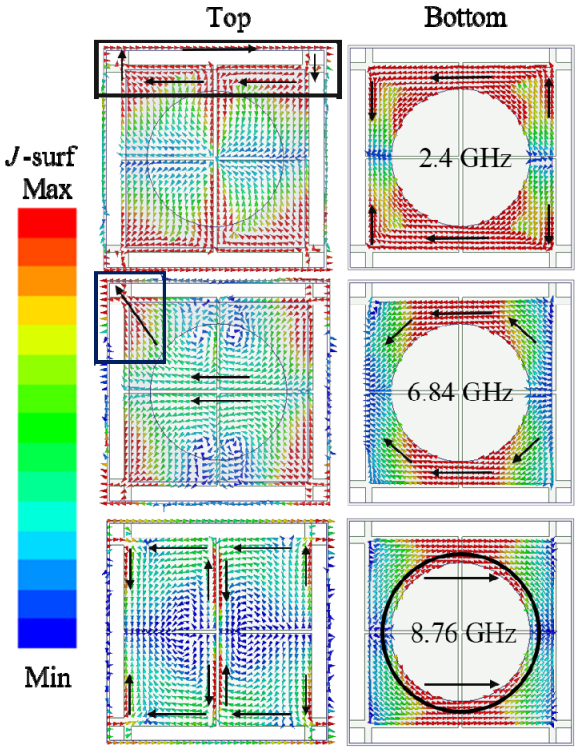

FIGURE 4. Surface current distributions of the proposed FSS at 2.4 GHz, 6.84 GHz and 8.76 GHz under TE polarization.

polarization-independent, angular-stable and wide stopband performance.

FSS prototype is fabricated and measured with 33 × 33 cells for verification. The photograph is displayed in Fig. 6. The scattering parameters of the proposed FSS are measured by an ENA Series Network Analyzer (Agilent E5072A, 30 kHz-8.5 GHz) and two horn antennas in a microwave anechoic chamber. To ensure the accuracy of the experiment, the measurement was implemented by three steps: First, connect two horn antennas to the Network Analyzer using two cables; Second, calibrate (though) the antennas and cables after aligning two antennas (transmission coefficient should be a straight line at 0 dB if the calibration is successful); Third, put the FSS between two antennas, and then save the data directly. Note that time-domain gate can be set up in the Network Analyzer if you want to test more accurately.

Simulated and measured scattering parameters are depicted in Fig. 6 under normal incidence in the case of TE and TM polarizations. It is found that the measured results agree well with the simulated ones. The simulated -3 dB bandwidth for the passband at 2.4 GHz is 28.2% from 2.01 to 2.67 GHz, while the measured one is 23.5% from 2.14 to 2.71 GHz. The simulated bandstop response covers a frequency spectrum of 3.35-9.4 GHz (94.9%). Owing to the limitation of the frequency range of Network Analyzer, our maximum test frequency can only reach 8.5 GHz. Nevertheless, the proposed FSS could achieve wide stopband performance from the trend of measurement curve.

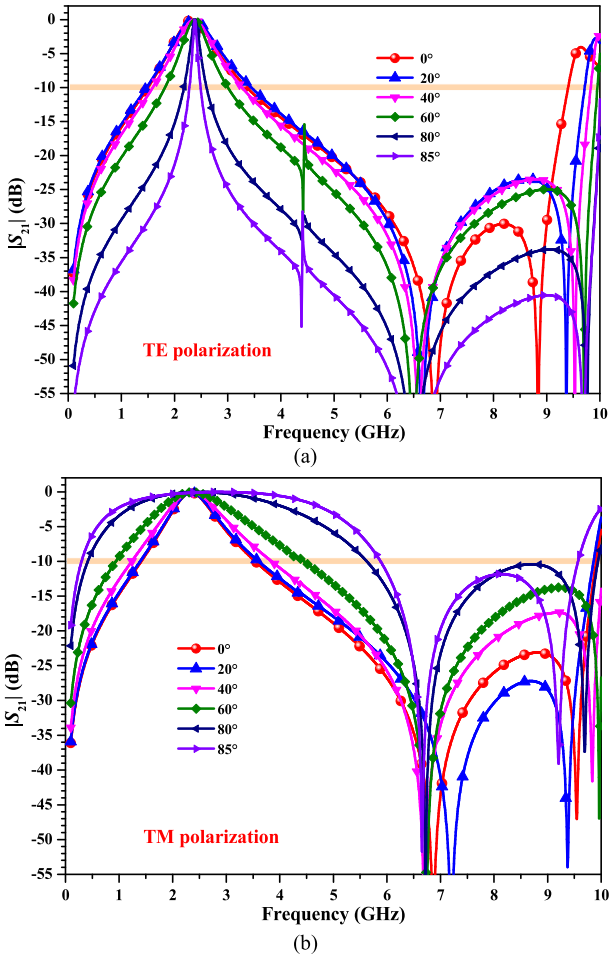

FIGURE 5. Simulated transmission coefficients of the proposed FSS for various incident angles ranging from 0° to 88° under (a) TE, and (b) TM polarization.

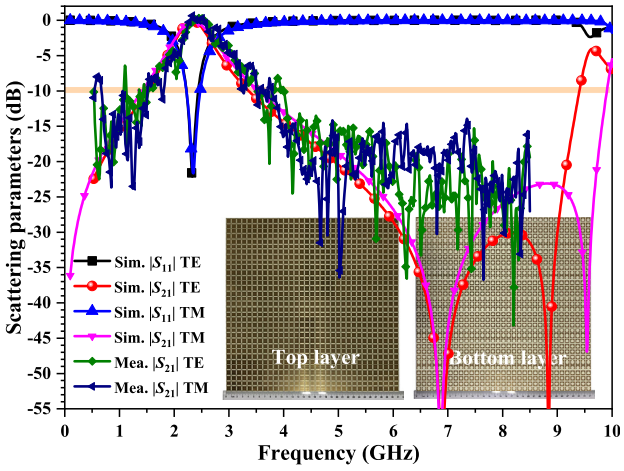

FIGURE 6. Simulated and measured scattering parameters under normal incidence.

Additionally, there is a stable transmissive window from the measured results at 2.4 GHz.

To sum up, the proposed FSS has numerous advantages such as miniaturization, angular stable and wide stopband. Meanwhile, two resonant points in the rejection band can

TABLE 1. The performance comparison.

Refs	Year	Size	Miniaturization technique	Angular stability	Upper stopband
[6]	2014	$0.045\lambda_0 \times 0.096\lambda_0$	3-D structure	60°	Suppress up to $9f_0$
[7]	2019	$0.056\lambda_0 \times 0.056\lambda_0$	3-D printing	75°	One transmission zero
[8]	2018	$0.107\lambda_0 \times 0.107\lambda_0$	Loading with Lumped reactive components	N.A.	One transmission zero
[9]	2019	$0.035\lambda_0 \times 0.035\lambda_0$	Loading with capacitive structures (convoluted slot grids)	60°	N.A.
[10]	2018	$0.094\lambda_0 \times 0.094\lambda_0$	Multilayer substrate stacking technology	60°	$\lvert S_{21} \leq$-20dB$\rvert$: 5.86 -14.9 GHz
[11]	2013	$0.3\lambda_0 \times 0.3\lambda_0$	Cascading two loop arrays	40°	Two transmission zeros
[12]	2019	$0.645\lambda_0 \times 0.645\lambda_0$	Cascading two arrays (hollow metal pipe and metal disk)	Not suitable for oblique incidence	Two independent adjustable transmission zeros
This paper		**$0.0756\ \lambda_0 \times 0.0756\ \lambda_0$**	**Increasing capacitance by introducing gaps (Metasurface)**	**80°**	**Two independent adjustable transmission zeros**

N.A.: No specific values.

be tuned independently. Hence, the proposed FSS can be applied in the communication systems to improve signal-to-noise ratio in the passband and reduce out-of-band noise. To highlight the advantages of the proposed FSS, performance comparisons between the proposed FSS and other designs in the previous literature are provided in TABLE 1.

IV. CONCLUSION

This paper reports a dual-polarized FSS based on metasurface with angular-stable and wide rejection band function. Meanwhile, there is a transmission window with low insertion loss at 2.4 GHz. When the proposed FSS is illuminated by electromagnetic wave, the scattering parameters perform stable under different incident angles up to 80° for both TE and TM polarization. This is because the miniaturization of the unit-cell inhibits the generation of grate lobes. The equivalent circuit is also presented to explain the operation mechanism of the proposed FSS. It is proved that two resonant points in stopband could also be tuned independently. Namely, the bandwidth of stopband could be adjusted easily. Therefore, the proposed FSS could be employed in 2.4 GHz wireless local area network application. The simulated and measured results both validate its versatility and feasibility.

REFERENCES

[1] S. Narayan, G. Gulati, B. Sangeetha, and R. U. Nair, "Novel metamaterial-element-based FSS for airborne radome applications," *IEEE Trans. Antennas Propag.*, vol. 66, no. 9, pp. 4695–4707, Sep. 2018.

[2] H. Zhou, S. Qu, B. Lin, J. Wang, H. Ma, Z. Xu, W. Peng, and P. Bai, "Filter-antenna consisting of conical FSS radome and monopole antenna," *IEEE Trans. Antennas Propag.*, vol. 60, no. 6, pp. 3040–3045, Jun. 2012.

[3] V. Krushna Kanth and S. Raghavan, "EM design and analysis of frequency selective surface based on substrate-integrated waveguide technology for airborne radome application," *IEEE Trans. Microw. Theory Techn.*, vol. 67, no. 5, pp. 1727–1739, May 2019.

[4] N. Liu, X. Sheng, C. Zhang, and D. Guo, "Design of frequency selective surface structure with high angular stability for radome application," *IEEE Antennas Wireless Propag. Lett.*, vol. 17, no. 1, pp. 138–141, Jan. 2018.

[5] M. Qu, S. Sun, L. Deng, and S. Li, "Design of a frequency-selective rasorber based on notch structure," *IEEE Access*, vol. 7, pp. 3704–3711, 2019.

[6] H. Huang and Z. Shen, "Absorptive frequency-selective transmission structure with square-loop hybrid resonator," *IEEE Antennas Wireless Propag. Lett.*, vol. 16, pp. 3212–3215, 2017.

[7] Z. Wang, Q. Zeng, J. Fu, W. Chen, B. Lv, M. Song, and T. A. Denidni, "A high-transmittance frequency-selective rasorber based on dipole arrays," *IEEE Access*, vol. 6, pp. 31367–31374, 2018.

[8] Q. Chen, D. Sang, M. Guo, and Y. Fu, "Frequency-selective rasorber with interabsorption band transparent window and interdigital resonator," *IEEE Trans. Antennas Propag.*, vol. 66, no. 8, pp. 4105–4114, Aug. 2018.

[9] G.-B. Wu, S.-W. Qu, Y.-X. Wang, and S. Yang, "Nonuniform FSS-backed reflectarray with synthesized phase and amplitude distribution," *IEEE Trans. Antennas Propag.*, vol. 66, no. 12, pp. 6883–6892, Dec. 2018.

[10] M. L. Zimmerman, S. W. Lee, and G. Fujikawa, "Analysis of reflector antenna system including frequency selective surfaces," *IEEE Trans. Antennas Propag.*, vol. 40, no. 10, pp. 1264–1266, Oct. 1992.

[11] S. Mohamad, R. Cahill, and V. Fusco, "Performance of archimedean spiral antenna backed by FSS reflector," *Electron. Lett.*, vol. 51, no. 1, pp. 14–16, Jan. 2015.

[12] R. V. S. R. Krishna and R. Kumar, "Slotted ground microstrip antenna with FSS reflector for high-gain horizontal polarisation," *Electron. Lett.*, vol. 51, no. 8, pp. 599–600, Apr. 2015.

[13] F. Bayatpur and K. Sarabandi, "Multipole spatial filters using metamaterial-based miniaturized-element frequency-selective surfaces," *IEEE Trans. Microw. Theory Techn.*, vol. 56, no. 12, pp. 2742–2747, Dec. 2008.

[14] X. Zhang, "Terahertz filter based on frequency selective surfaces," *Adv. Mater. Res.*, vol. 571, pp. 362–366, Sep. 2012.

[15] M. H. Nisanci, A. Y. Tesneli, N. B. Tesneli, F. Ustuner, E. Demirel, F. de Paulis, and A. Orlandi, "Notice of retraction: Experimental validation of a 3D FSS designed by periodic conductive fibers part-1: Band-pass filter characteristic," *IEEE Trans. Electromagn. Compat.*, vol. 59, no. 6, pp. 1841–1847, Dec. 2017.

[16] M. H. Nisanci, N. B. Tesneli, A. Y. Tesneli, F. Ustuner, E. Demirel, F. de Paulis, and A. Orlandi, "Notice of retraction: Experimental validation of a 3D FSS designed by periodic conductive fibers part-2: Band-stop filter characteristic," *IEEE Trans. Electromagn. Compat.*, vol. 59, no. 6, pp. 1835–1840, Dec. 2017.

[17] M. Hajj, E. Rodes, and T. Monediere, "Dual-band EBG sectoral antenna using a single-layer FSS for UMTS application," *IEEE Antennas Wireless Propag. Lett.*, vol. 8, pp. 161–164, 2009.

[18] C. Huang, C. Ji, X. Wu, J. Song, and X. Luo, "Combining FSS and EBG surfaces for high-efficiency transmission and low-scattering properties," *IEEE Trans. Antennas Propag.*, vol. 66, no. 3, pp. 1628–1632, Mar. 2018.

[19] E. Rodes, M. Diblanc, E. Arnaud, T. Monediere, and B. Jecko, "Dual-band EBG resonator antenna using a single-layer FSS," *IEEE Antennas Wireless Propag. Lett.*, vol. 6, pp. 368–371, 2007.
[20] B. Li and Z. Shen, "Bandpass frequency selective structure with wide-band spurious rejection," *IEEE Antennas Wireless Propag. Lett.*, vol. 13, pp. 145–148, 2014.
[21] S. Ghosh and S. Lim, "A miniaturized bandpass frequency selective surface exploiting three-dimensional printing technique," *IEEE Antennas Wireless Propag. Lett.*, vol. 18, no. 7, pp. 1322–1326, Jul. 2019.
[22] N. Liu, X. Sheng, C. Zhang, J. Fan, and D. Guo, "A design method for synthesizing miniaturized FSS using lumped reactive components," *IEEE Trans. Electromagn. Compat.*, vol. 60, no. 2, pp. 536–539, Apr. 2018.
[23] P.-C. Zhao, Z.-Y. Zong, W. Wu, B. Li, and D.-G. Fang, "Miniaturized-element bandpass FSS by loading capacitive structures," *IEEE Trans. Antennas Propag.*, vol. 67, no. 5, pp. 3539–3544, May 2019.
[24] B. Li, X. Huang, L. Zhu, Y. Zhang, Y. Tang, W.-J. Lu, and Y. Bo, "Bandpass frequency selective structure with improved out-of-band rejection using stacked single-layer slotlines," *IEEE Trans. Antennas Propag.*, vol. 66, no. 11, pp. 6003–6014, Nov. 2018.
[25] B. Li and Z. Shen, "Synthesis of quasi-elliptic bandpass frequency-selective surface using cascaded loop arrays," *IEEE Trans. Antennas Propag.*, vol. 61, no. 6, pp. 3053–3059, Jun. 2013.
[26] Z. Zhao, A. Zhang, X. Chen, G. Peng, J. Li, H. Shi, and A. A. Kishk, "Bandpass FSS with zeros adjustable quasi-elliptic response," *IEEE Antennas Wireless Propag. Lett.*, vol. 18, no. 6, pp. 1184–1188, Jun. 2019.
[27] P.-C. Zhao, Z.-Y. Zong, W. Wu, B. Li, and D.-G. Fang, "An FSS structure with geometrically separable meander-line inductors and parallel-plate capacitors," *IEEE Trans. Antennas Propag.*, vol. 65, no. 9, pp. 4693–4705, Sep. 2017.

MEIJUN QU received the B.S. degree from the College of Physics and Electronics, Shanxi University, Taiyuan, China, in 2015. She is currently pursuing the Ph.D. degree with the School of Information and Communication Engineering, Beijing University of Posts and Telecommunications (BUPT), Beijing, China. Her research interests include microwave passive component, antenna, metamaterial, and electromagnetic compatibility.

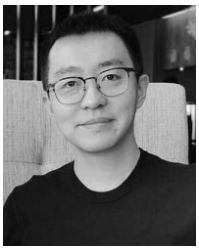

BIN LI is currently an Engineer with the International Department, The State Radio Monitoring Center Testing Center. He is mainly engaged in SAR, MIMO OTA, and 5G terminal testing, standard setting and related technology research.

SIYANG SUN is currently an Associate Professor with the China Telecommunication Technology Labs, China Academy of Information and Communications Technology. As an Antenna Research and Development Engineer, he participated in many national scientific research projects, was responsible for the development and testing of antenna systems, completed the design, commissioning and testing of various antennas (arrays), and successfully applied them in many projects. As a Project Director Designer, he was responsible for the coordination, communication, document writing, debugging, and testing of the project. He has published more than ten academic articles and applied for a national defense patent. He is mainly engaged in MIMO OTA and 5G terminal testing, standard setting, and related technology research.

SHUFANG LI (Senior Member, IEEE) received the Ph.D. degree from the Department of Electrical Engineering, Tsinghua University, Beijing, China, in 1997. She is currently the Director of the Ubiquitous Electromagnetic Environment Center of Education Ministry, China, and the Director of the Joint Laboratory, BUPT, and The State Radio Monitoring Center (SRMC), China. She has published hundreds of articles interiorly and overseas, as well as several textbooks, translation works, and patents. Her research interests include the theory and design technology of radio frequency circuits in wireless communications, EMI/EMC, and simulation technology and optimization for radiation interfere on high-speed digital circuit. She received the Young Scientists Reward sponsored by the International Union of Radio Science (URSI).